THE UNIVERSITY *of* EDINBURGH

Edinburgh Research Explorer

Knudsen heat capacity

OPEN ACCESS

Knudsen heat capacity

Gulru Babac[1,a)] and Jason M. Reese[2]

[1]*Institute of Energy, Istanbul Technical University, Istanbul 34469, Turkey*
[2]*School of Engineering, University of Edinburgh, Edinburgh EH9 3JL, United Kingdom*

We present a "Knudsen heat capacity" as a more appropriate and useful fluid property in micro/nanoscale gas systems than the constant pressure heat capacity. At these scales, different fluid processes come to the fore that are not normally observed at the macroscale. For thermodynamic analyses that include these Knudsen processes, using the Knudsen heat capacity can be more effective and physical. We calculate this heat capacity theoretically for non-ideal monatomic and diatomic gases, in particular, helium, nitrogen, and hydrogen. The quantum modification for para and ortho hydrogen is also considered. We numerically model the Knudsen heat capacity using molecular dynamics simulations for the considered gases, and compare these results with the theoretical ones. © *2014 AIP Publishing LLC*. [http://dx.doi.org/10.1063/1.4872335]

I. INTRODUCTION

The development of thermodynamic and transport models for micro/nanoscale fluid systems has received a great deal of attention in recent years, e.g., Refs. 1–4. Several physical effects become important in these systems that are generally ignored in macroscale systems, such as thermal creep,[5,6] quantum size effects,[7,8] and thermosize effects.[9–12]

Analysis of temperature-driven rarefied gas flows between two reservoirs at temperatures T_H (hot) and T_L (cold), and at pressures p_H and p_L, leads to the temperature-pressure relation $p_H/\sqrt{T_H} = p_L/\sqrt{T_L}$.[5,6] This relation is called the "Knudsen law" and it has been investigated extensively in the literature for micro/nanoscale systems in connection with thermal creep and the Knudsen pump or compressor. According to this relation, for a temperature-driven gas flow at the micro/nanoscale, the constant parameter in the flow is $p/\sqrt{T}$, therefore the process can be called a $p/\sqrt{T}$ constant process (a Knudsen process), and $\vec{\nabla}\left(p/\sqrt{T}\right) = 0$. This is analogous to a constant pressure process at the macroscale.

The Knudsen law can also affect thermodynamic properties. In some reports of thermodynamic gas cycles,[10,11] incorporating a Knudsen process within a thermodynamic cycle can open up new cycle design and introduce some differences from the conventional thermodynamic analysis, for example, in the constant pressure heat capacities that are generally used in the continuum-fluid limit.

In this paper, we present a detailed analysis of the heat capacity in a micro/nanoscale gas system. We show that, instead of the conventional constant pressure heat capacity, a heat capacity that incorporates the Knudsen process — which we call the "Knudsen heat capacity" — is appropriate. We present molecular dynamics (MD) simulations of various nanoscale gas flows, and heat capacity measurements from these simulations for monatomic and polyatomic gases. These measurements are compared with the theoretical solutions. Our results show that the Knudsen heat capacity is a more useful fluid property than the conventional heat capacity in gas flows that follow the Knudsen law.

---

a)Author to whom correspondence should be addressed. Electronic mail: babac@itu.edu.tr

II. THE KNUDSEN PROCESS

A temperature-driven gas flow in a macro channel is dominated by hydrodynamic flow behavior: molecule-molecule collisions determine the gas properties under the applied temperature gradient. At steady state, this is a constant pressure process, i.e., $\vec{\nabla} p = 0$, which can be easily shown through the conventional Navier-Stokes equations. In a thermodynamic analysis, the ratio of the amount of transferred heat energy to the imposed temperature difference along the channel requires the heat capacity for a constant pressure process, C_p.

On the other hand, a gas flow driven by a temperature gradient in a micro or nano channel can be dominated by free-molecular, or close to free-molecular, flow behavior in which molecule-wall collisions mainly determine the gas properties. At steady state, the zero net flux condition results in the following equation relating the pressure to the temperature in the system:[13]

$$\frac{1}{p}\frac{\partial p}{\partial x} = \gamma \frac{1}{T}\frac{\partial T}{\partial x}, \tag{1}$$

where x is the direction along the channel, and γ is a function of the rarefaction parameter and depends on the geometry, molecule-surface interaction, type of gas etc.[14] When Equation (1) is integrated along the channel from the hot (T_H) to the cold (T_L) temperature ends, and the Knudsen number variation is ignored, the constant process in this micro or nano domain can be written as $\vec{\nabla}(p/T^\gamma) = 0$. The familiar Knudsen equation can be obtained from this equation in the free-molecular limit by setting $\gamma = 0.5$ so that $\vec{\nabla}\left(p/\sqrt{T}\right) = 0$.

III. KNUDSEN HEAT CAPACITY FOR IDEAL GASES

The ratio of the amount of heat energy transferred, to the imposed temperature difference along the channel, is the heat capacity for the constant process in free molecular flows that are defined by $\vec{\nabla}\left(p/\sqrt{T}\right) = 0$. We term this the "Knudsen heat capacity," $C_{p/\sqrt{T}}$.

A heat capacity can be calculated by taking the temperature derivative of the entropy, S, in a constant process, i.e.,

$$C_{\text{cons. proc.}} = T\left(\frac{dS}{dT}\right)_{\text{cons. proc.}} . \tag{2}$$

The entropy for ideal gases can be obtained from the Helmholtz free energy, $F = -Nk_BT \ln Z$, where k_B is the Boltzmann constant, N is the number of molecules, and Z is the partition function. Considering only translational modes, $Z = Z_{trans} = V^N (2\pi mk_BT)^{3N/2}/N!h^{3N}$, where m is the molecular mass, and h is the Planck constant. Therefore, the entropy per molecule, s, can be written as

$$s = \frac{S}{N} = -\left(\frac{dF}{dT}\right)_V = k_B\ln\left(\frac{Ak_BT^{5/2}}{p}\right) + \frac{5k_B}{2}, \tag{3}$$

where A is a constant given by $A = (2\pi mk_B)^{3/2}/h^3$. By substituting Eq. (3) into Eq. (2) and taking derivatives under the conditions of constant pressure and of a Knudsen process, the heat capacities per molecule can be obtained as follows:

$$c_p = \frac{C_p}{N} = 5k_B/2, \tag{4}$$

$$c_{p/\sqrt{T}} = \frac{C_{p/\sqrt{T}}}{N} = 2k_B, \tag{5}$$

for monatomic ideal gases. In other words, when a temperature-driven gas flow in the free molecular flow regime is considered, the heat capacity in the process should be assessed as $c_{p/\sqrt{T}} = 2k_B$, instead of $c_p = 5k_B/2$, because of the Knudsen law. In free molecular flow-dominated systems, such as at the micro/nanoscale, using the Knudsen heat capacity should give more accurate results than using the constant pressure heat capacity that is more appropriate for classical thermofluid systems.

As discussed in Sec. II, the pressure drop in a rarefied gas flow depends on γ, through Eq. (1). The heat capacity can be generalized accordingly, in order to encompass the hydrodynamic regime to the free molecular flow regime, as

$$c_{p/T^\gamma} = \left(\frac{5}{2} - \gamma\right) k_B, \tag{6}$$

where γ is 0 or 1/2 for the hydrodynamic or the free molecular flow regimes, respectively.

The parameter γ depends on many factors, but significantly for our purposes it depends on the Knudsen number Kn.[14] The relation between Kn and γ has been generally discussed in the literature for two limiting cases: hydrodynamic flow ($Kn \to 0$), and free molecular flow ($Kn \to \infty$).[15–17] In the $Kn \to 0$ limit, the heat capacity is already known to be $c_p = 5k_B/2$. As $Kn \to \infty$, γ converges to 0.5, with the deviation from this value decreasing with increasing Knudsen number. Therefore, for free molecular flow γ can be set directly to be 0.5 and the Knudsen heat capacity can be obtained as $c_{p/\sqrt{T}} = 2k_B$, as discussed above.

For the flow characteristic dependency of the heat capacity, we need a more general relation between Kn and γ that can cover mid-range Knudsen numbers, however, the Kn-γ relations proposed in the literature are not always successful for these systems.[15–17] Because of the lack of a well-developed analytical expression for the Kn-γ relation over all flow regimes from the hydrodynamic to the free molecular, we have curve-fitted a relationship from data in the literature,[14, 18, 19] as follows.

In Refs. 14, 18, and 19, rarefied gas flows at different Knudsen numbers in different geometries were investigated using the S-model,[14] the BGK model,[18] and the hard-sphere gas model.[19] The γ relation can be obtained from logarithmic curve fitting to this published data in the range $Kn = 0.1$–10, i.e.,

$$\gamma = c_1 \ln(Kn) + c_2, \tag{7}$$

where c_1 and c_2 are coefficients determined by the curve fitting. The corresponding coefficients and R^2 values for each reported case are presented in Table I. Note that Eq. (7) does not converge in the limit $Kn \to \infty$, so for this limit case it is better to use other relations in the literature.[15–17] However, here we choose Knudsen numbers in the range Kn = 0.1–10 and continue with Eq. (7).

With Eq. (7), the heat capacity can be written as a function of the Knudsen number Kn, i.e.,

$$c_{p/T^\gamma} = \left(\frac{5}{2} - (c_1 \ln(Kn) + c_2)\right) k_B, \tag{8}$$

which is plotted in Figure 1 for the various coefficients in Table I. The heat capacity is 5/2 in the hydrodynamic limit, and with increasing Kn the heat capacity decreases. In free molecular flow conditions, $c_{p/T^\gamma}/k_B$ reaches the values at $Kn = 10$ of 1.99051 for Sharipov,[14] 2.01725 for Loyalka,[18] and 2.04608 for Ohwada et al.[19] These are reasonably close to the theoretical value of $c_{p/T^\gamma}/k_B = 2$ that we calculated above.

In Secs. IV A and IV B, this heat capacity will be investigated in detail for both monatomic and diatomic real gases. In Sec. V the Kn-dependency of the heat capacity is also analyzed using molecular dynamics simulations of gas flow in a nanoscale channel. Molecular dynamics simulates atomistic or molecular interactions and movements directly through Newton's laws. For the intermolecular interactions, the Lennard-Jones (LJ) potential is often used. Some phenomena that are usually ignored in the theoretical calculations, such as the effects of inlets/outlets at the ends of the domain, can be taken into account in MD simulations.

TABLE I. Fitting coefficients c_1, c_2, and corresponding R^2 values, for the Kn-γ relation.

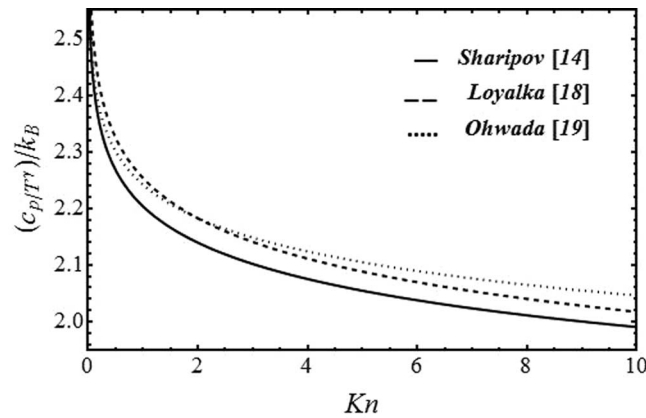|	c_1	c_2	R^2
Sharipov[14]	0.0925	0.2965	0.9782
Loyalka[18]	0.1026	0.2465	0.9853
Ohwada et al.[19]	0.0850	0.2582	0.9744

FIG. 1. Various heat capacity predictions varying with Knudsen number, *Kn*.

In our MD simulation reported in Sec. V below, the temperature gradients are kept in the mid- to low-temperature range so that the vibrational modes of the molecules are not excited. Therefore, the vibrational contribution to the heat capacities can be ignored in this analysis. The rotational and translational contributions are taken into account for diatomic cases, while only the translational contribution is considered for the monatomic case.

IV. KNUDSEN HEAT CAPACITY FOR REAL GASES

A. Monatomic gases

The Knudsen heat capacity for monatomic real gases is calculated by only considering the translational motion of the molecules. The partition function for translational motion can be written as

$$Z = Z_{trans} = \frac{1}{N!} \left(\frac{2\pi m k_B T}{h^2} \right)^{3N/2} V^N \left(1 - \frac{N^2}{V} b(T) \right), \tag{9}$$

where $b(T)$ is the second virial coefficient that is calculated depending on the intermolecular potential $U(r)$ through

$$b(T) = 2\pi \int\limits_0^\infty \left(1 - \exp\left(\frac{-U(r)}{k_B T} \right) \right) r^2 dr. \tag{10}$$

A LJ potential can be used, viz.,

$$U_{LJ} = 4\varepsilon \left[\left(\frac{\sigma}{R_{ij}} \right)^{12} - \left(\frac{\sigma}{R_{ij}} \right)^6 \right], \tag{11}$$

where ε is the depth of the intermolecular potential well, σ is the finite distance at which the intermolecular potential is zero, and R_{ij} is the distance between molecules i and j. The LJ parameters for the gases we consider are discussed below.

The entropy and Knudsen heat capacity per molecule for real gases are then calculated as

$$s = \frac{5k_B}{2} + k_B \ln \left[\frac{A k_B T^{5/2}}{p} \right] - p b'(T), \tag{12}$$

$$c_{p/\sqrt{T}} = T \left(\frac{ds}{dT} \right)_{p/\sqrt{T}} = 2k_B - \frac{p}{2} b'(T) - pT b''(T), \tag{13}$$

TABLE II. Constant pressure and Knudsen heat capacities calculated for some monatomic gases.

| Gas | LJ parameters[20] | | Molecular mass $m/10^{-27}$ (kg) | Calculated constant pressure heat capacity c_p/m (J/kg K) | Calculated Knudsen heat capacity $(c_{p/\sqrt{T}})/m$ (J/kg K) |
	ε/k_B (K)	σ (Å)			
He	10.2	2.576	6.646	5190	4152
Ne	35.7	2.789	33.509	1029	823
Ar	124	3.418	66.336	521	417
Kr	225	3.498	139.153	249	199
Xe	229	4.055	218.012	159	127

where the pressure defined for real gases is $p = nk_B T/(1 - nb(T))$. Here, $b'(T)$ and $b''(T)$ are the first and second derivatives of $b(T)$ with respect to T, respectively. If we were to consider a macro channel gas flow under the same conditions, we should use the constant pressure heat capacity for real gases, which is defined per molecule as

$$c_p = T \left(\frac{ds}{dT} \right)_p = \frac{5}{2} k_B - pT b''(T). \tag{14}$$

Equations (13) and (14) can be compared for monatomic real gases. We perform this comparison for Ne, Ar, Kr, Xe, and He gases at standard conditions (i.e., at 300 K and 1 atm), and this is presented in Table II. (Values are presented per unit mass, by dividing Eqs. (13) and (14) by the molecular mass.)

As can be seen from Table II, the constant pressure heat capacity in the hydrodynamic regime is some 20% higher than the Knudsen heat capacity in the free molecular regime. So using the constant pressure heat capacity instead of the Knudsen heat capacity when considering micro/nanoscale free molecular (or close to free molecular) flows may introduce a significant error into the results and thermodynamic analyses.

In Table II, c_p and $c_{p/\sqrt{T}}$ represent the two limiting transport cases. The heat capacity for real gases can be generalized using γ in order to cover slip and translational flows as well, i.e.,

$$c_{p/T^\gamma} = \left(\frac{5}{2} - \gamma \right) k_B - p\gamma b'(T) - pT b''(T). \tag{15}$$

If Eq. (7) is substituted into Eq. (15), with coefficients from Table I, the best match with the calculated Knudsen heat capacities in Table II is obtained for He and Ne gases. Using the coefficients of Sharipov's data[14] from Table I, the values of heat capacity are within about 5% for both the low and high Knudsen number cases; for the coefficients from Loyalka,[18] heat capacities are within 2% for low Knudsen numbers and about 4.5% for high Knudsen number cases; and for the coefficients from Ohwada *et al.*,[19] within 2.5% for low Knudsen numbers, and within 7.5% for high Knudsen numbers. The best match seems to be obtained using the coefficients from Loyalka's[18] data, especially for low *Kn*. For high *Kn*, both Sharipov's[14] and Loyalka's[18] data capture the heat capacities within about 5%. The differences between the results slightly increase for Ar, Kr, and Xe because of deviation from the ideal gas approximation for larger atoms.

B. Diatomic gases

For diatomic gases, the rotational contribution to the partition function should also be considered, i.e.,[21]

$$Z_{rot} = \sum_{l=0,1,\ldots} (2l + 1) \exp \left[-l(l + 1) \Phi/T \right], \tag{16}$$

where Φ is the characteristic temperature for rotation and l is the rotational energy level. If $T \gg \Phi$ the summation can be replaced with an integral, and the rotational partition function is $Z_{rot} = T/\Phi$.[21] The rotational contribution to the conventional constant pressure heat capacity makes $c_p = c_{p, trans}$

$+ c_{p,rot} = 5k_B/2 + k_B = 7k_B/2$ for an ideal gas. The characteristic temperature Φ is generally low for many gases, except for H_2. Therefore, the $T \gg \Phi$ assumption can often be used[21] and under this assumption the entropy and Knudsen heat capacity for real diatomic gases take the following forms:

$$s = \frac{7k_B}{2} + k_B \ln \left[\frac{A k_B T^{7/2}}{p\Phi} \right] - pb'(T), \tag{17}$$

$$c_{p/\sqrt{T}} = T \left(\frac{ds}{dT} \right)_{p/\sqrt{T}} = 3k_B - \frac{p}{2}b'(T) - pTb''(T). \tag{18}$$

The constant pressure heat capacity for diatomic real gases is

$$c_p = T \left(\frac{ds}{dT} \right)_p = \frac{7}{2}k_B - pTb''(T). \tag{19}$$

These can be generalized using γ, as before, to give

$$c_{p/T^\gamma} = \left(\frac{7}{2} - \gamma \right) k_B - p\gamma b'(T) - pTb''(T). \tag{20}$$

The heat capacities for common gases such as N_2 and O_2 can then be calculated for free molecular flows and hydrodynamic flows by using Eqs. (18) and (19), respectively. For 300 K and 1 atm, this results in $\left(c_{p/\sqrt{T}} \right)_{N_2} = 890$ J/kg K and $\left(c_{p/\sqrt{T}} \right)_{O_2} = 779$ J/kg K; $(c_p)_{N_2} = 1039$ J/kg K and $(c_p)_{O_2} = 909$ J/kg K, where the required Lennard-Jones parameters are $\sigma_{N_2} = 3.3$ Å and $(\varepsilon/k_B)_{N_2} = 36$ K; $\sigma_{O_2} = 3.1062$ Å and $(\varepsilon/k_B)_{O_2} = 43.183$ K.[22]

For H_2 gas, $T \gg \Phi$ cannot be assumed, therefore, Eqs. (17)–(20) cannot be used. The rotational partition function in Eq. (16) should be rewritten by considering ortho and para hydrogen (which correspond to symmetric and antisymmetric wave functions for even and odd values of l), and this is given in Ref. 21 as

$$Z_{rot-H_2} = \sum_{l=even.} (2l+1) \exp\left[-l(l+1)\Phi/T\right] + 3 \sum_{l=odd} (2l+1) \exp\left[-l(l+1)\Phi/T\right]. \tag{21}$$

The rotational contribution to heat capacity can then be incorporated into the Knudsen and constant pressure heat capacities, respectively, and leads to

$$c_{p/\sqrt{T}} = 2k_B - \frac{p}{2}b'(T) - pTb''(T) + 2k_BTf'(T) + T^2 k_B f''(T), \tag{22}$$

$$c_p = \frac{5}{2}k_B - pTb''(T) + 2k_BTf'(T) + T^2 k_B f''(T), \tag{23}$$

with the general form of the hydrogen heat capacity

$$c_{p/T^\gamma} = \left(\frac{5}{2} - \gamma \right) k_B - p\gamma b'(T) - pTb''(T) + 2k_BTf'(T) + T^2 k_B f''(T), \tag{24}$$

where f is a function defined for ortho and para hydrogen,

$$f_{para}(T) = \ln \left[\sum_{l,even} (2l+1) \exp\left[-l(l+1)\Phi/T\right] \right], \tag{25}$$

$$f_{ortho}(T) = \ln \left[3 \sum_{l,odd} (2l+1) \exp\left[-l(l+1)\Phi/T\right] \right], \tag{26}$$

and f' and f'' are the first and second derivatives of f with respect to T, respectively. The heat capacities for para and ortho hydrogen can then be calculated at $p = 1$ atm, by taking the sums in Eqs. (25) and (26), respectively. The results are presented in Figure 2.
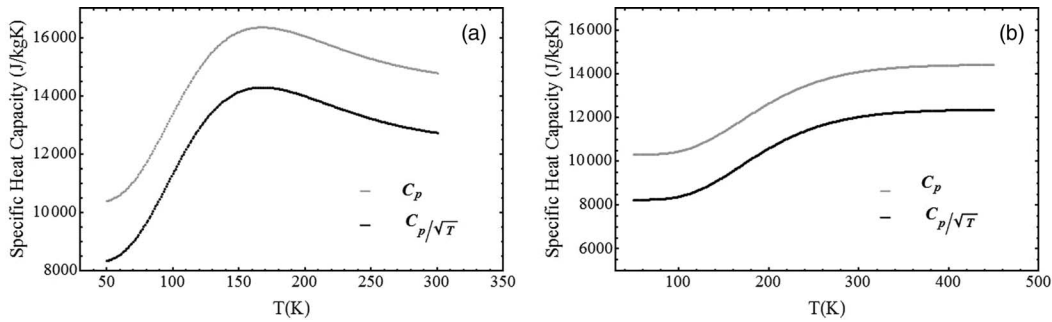
FIG. 2. Constant pressure (gray line) and Knudsen (black line) heat capacities at 1 atm, for (a) para hydrogen, and (b) ortho hydrogen.

Hydrogen gas is also simulated with MD in Sec. V; however, the quantum character of rotational motions is not included in these simulations, so only translational effects can be examined. The quantum corrections for para and ortho hydrogen calculations are subsequently added into our MD results using a separate numerical routine in order to obtain the full predictions of hydrogen heat capacities.

V. MOLECULAR DYNAMICS SIMULATIONS

We use MD simulations of temperature-driven gas flow in a nano channel in order to investigate the Knudsen heat capacity. The MD simulations are performed using the open source OpenFOAM software, which incorporates a parallelized non-equilibrium MD solver.[23–25] A schematic of the system we consider is shown in Figure 3.

A 2D nano channel is thermally in contact with hot (temperature of T_H) and cold (T_L) reservoirs. Berendsen thermostats, with a coupling parameter of 1 ps, are applied to keep the temperatures constant in the reservoirs.[26] As solid surface boundary conditions (BCs), diffusive wall, and diffusive wall with a linear temperature gradient, are applied along the y and x directions, respectively. The solid boundary accommodation coefficient is set to be 1. In the z direction, periodic BCs are used to ensure the effective two-dimensionality of the setup.

Simulations are run for monatomic and diatomic gases, and results are compared with the theoretical calculations. Helium and nitrogen gases are considered as exemplars of monatomic and diatomic gases. Hydrogen gas is also considered in a MD simulation, but, as outlined in Sec. IV, the heat capacity of H_2 depends on quantum effects and the ortho/para state, and these are not generally included in MD. So the contribution from the translational part is simulated using MD. Then the partition function, Eq. (21), and the para-ortho functions in Eqs. (25) and (26) are defined in Mathematica: summations are calculated and the rotational contribution to heat capacities is evaluated. Finally, the MD and Mathematica results are added together according to Eqs. (22)–(24).

We carry out simulations for $Kn = 0.2, 0.5, 0.75, 1, 2, 5, 7.5,$ and 10. For $Kn = 0.2$, the flow is in the slip regime,[2] not free molecular; therefore, the heat capacity values should be in between the constant pressure heat capacity and the Knudsen heat capacity. For $Kn = 10$, the flow is nearly
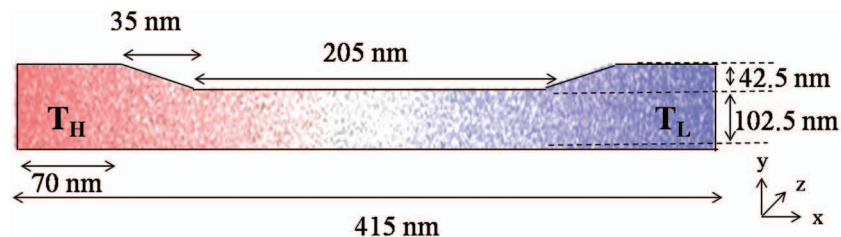

FIG. 3. Schematic of the nano channel for MD simulations.

TABLE III. Molecular parameters for the gases considered in our MD simulations. Values taken from Refs. 27–30.

|	Positions			Lennard-Jones parameters		Charge
	X (Å)	Y (Å)	Z (Å)	ε/k_b (K)	σ (Å)	q (e)
			Helium (He)			
He	0	0	0	10.2	2.576	0
			Nitrogen (N$_2$)			
N	0.549	0	0	36	3.3	-0.5075
N	-0.549	0	0	36	3.3	-0.5075
M	0	0	0	. . .	. . .	1.015
			Hydrogen (H$_2$)			
H	0.37	0	0	17.4	2.65	-0.489
H	-0.37	0	0	17.4	2.65	-0.489
M	0	0	0	. . .	. . .	0.978

in the free molecular regime, therefore the measured heat capacity should be close to the Knudsen heat capacity value. Temperature ranges for the simulations are determined according to the critical temperature of the gases, in order to maintain in gas phases throughout the simulations: 10–300 K for He, 30–300 K for H$_2$, and 110–300 K for N$_2$.

In our MD simulations, the molecules interact with each other via LJ and Coulomb potentials, for which the parameters are given in Table III.[27,30] The N$_2$ and H$_2$ molecules are represented with 3 sites as NNM and HHM, where M is a massless charged site to reproduce the polar nature of the molecule. The MD time step is around 2 fs, and the number of atoms in the system is kept at around 40 000–45 000 for all three gases. Each simulation runs in parallel on 16 cores for nearly a month.

VI. RESULTS AND DISCUSSION

The heat capacity is measured directly from the energy fluctuations in each MD simulation.[31] The measurements are made in the middle of the channel to eliminate inlet/outlet effects. The variations of the heat capacity of He and N$_2$ gases with Knudsen number are presented in Figure 4, which were obtained by running MD simulations of the system for different Kn numbers; $Kn = 0.2$, 0.5, 0.75, 1, 2, 5, 7.5, and 10. The profile of the results in Figure 4 is similar to that of the theoretical results in Fig. 1: the heat capacity decreases logarithmically with increasing Knudsen number.

The heat capacities for He and N$_2$ are also calculated with the model equations derived in this paper, and these are presented in Figs. 5 and 6, respectively. In each of these figures, the sub-figures are the heat capacity measurements for the same gases under the same temperature gradient, but for the different Knudsen numbers $Kn = 0.5$, 1, 5, and 10. The pressure and temperature measurements from the MD simulations are used in the model equations; the γ values are calculated
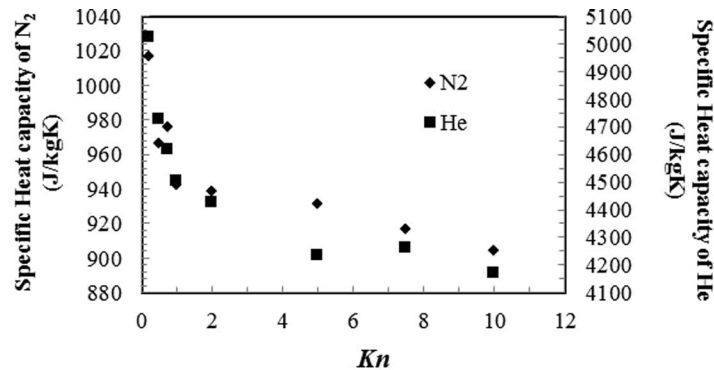
FIG. 4. The variation of the heat capacity of He and N$_2$ with Knudsen number, from MD simulations.
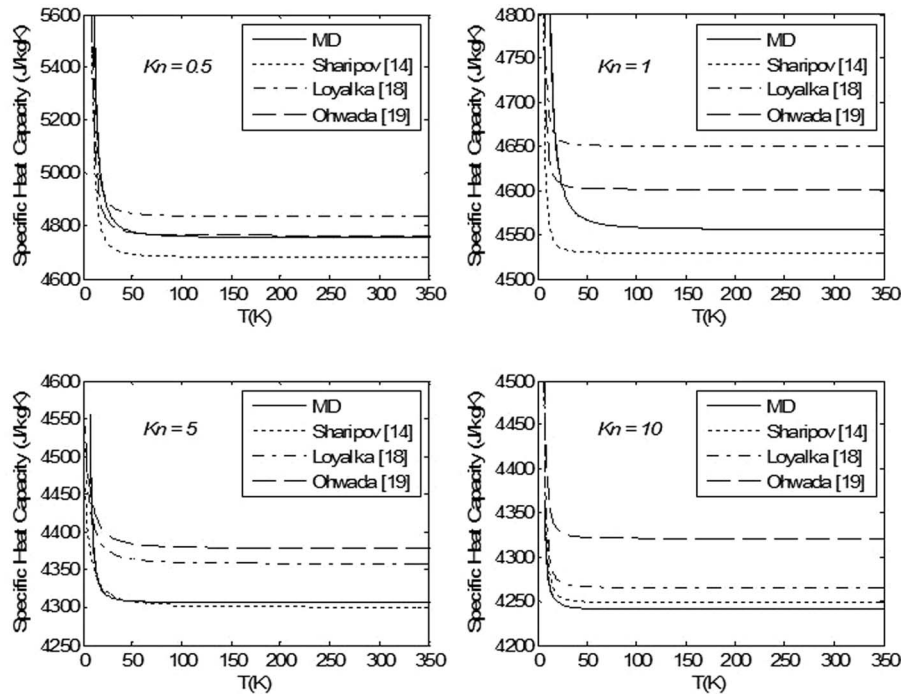
FIG. 5. Heat capacity of Helium for different Knudsen numbers, varying with temperature.

through $\gamma = \ln(p_2/p_1)/\ln(T_2/T_1)$ in our MD cases. Our MD results are compared with those in the literature.[14,18,19] Table IV presents the various values of γ reported in the literature and obtained from our MD simulations. By using these in Eq. (15) for the monatomic case and in Eq. (20) for the diatomic case, the plots of heat capacity versus T are obtained in Figs. 5 and 6.
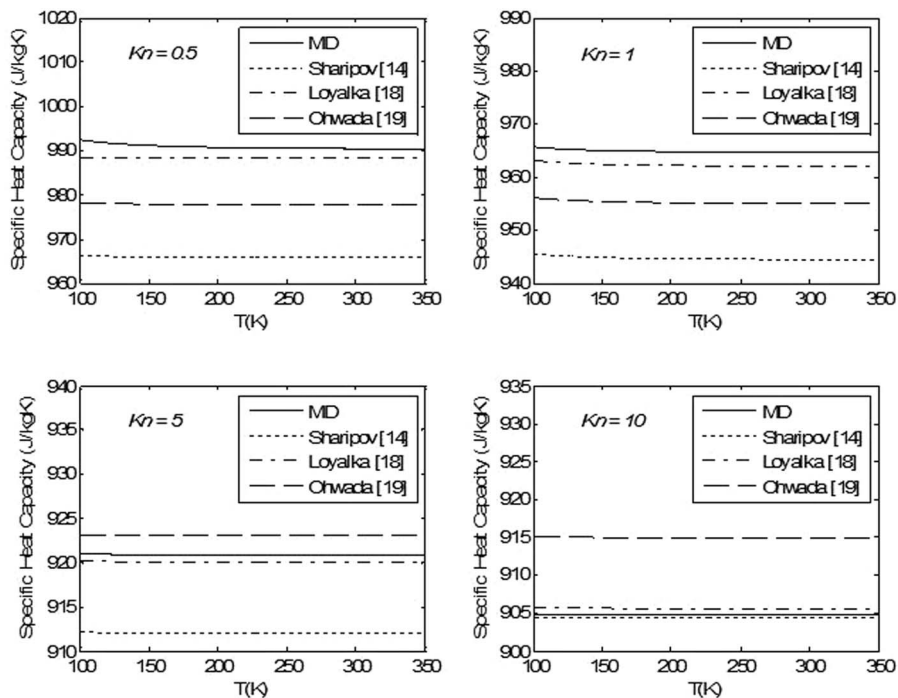

FIG. 6. Heat capacity of Nitrogen for different Knudsen numbers, varying with temperature.

TABLE IV. Reported γ values for various Kn.

	Sharipov[14]	Loyalka[18]	Ohwada et al.[19]	Our MD results for He	Our MD results for N_2
$Kn = 0.5$	0.2454	0.17	0.2053	0.2092	0.1635
$Kn = 1$	0.3179	0.2592	0.2825	0.3047	0.2538
$Kn = 5$	0.4273	0.4166	0.3912	0.4252	0.3974
$Kn = 10$	0.4532	0.4486	0.4175	0.4562	0.4520

In Figure 5, monatomic helium gas results for heat capacity are presented for $Kn = 0.5, 1, 5$, and 10. Because of the different transport processes, the heat capacity is different for different Kn. For $Kn = 10$, $Kn = 5$, and $Kn = 1$, the best agreement of our results is obtained with Sharipov's[14] data. The data of Loyalka[18] and Ohwada et al.[19] are consistently slightly above the MD results. However, for $Kn = 0.5$, the best agreement is obtained with the data of Ohwada et al.[19]

As a general observation regarding Figures 4 and 5, the heat capacity for He tends to the constant pressure heat capacity value at low Knudsen number, and tends towards the Knudsen heat capacity value with increasing Knudsen number, as can be checked from Table II. If the system could be simulated for lower and higher Knudsen numbers to get closer to hydrodynamic and free molecular conditions, respectively, the heat capacity values would also be closer to the values for the respective constant heat capacity and Knudsen heat capacity given in Table II as $(c_p)/m = 5190$ J/kg K and $(c_{p/\sqrt{T}})/m = 4152$ J/kg K, respectively.

A similar trend can also be seen for nitrogen gas in Figure 6, where comparison is made for different γ values within Eq. (20), the expression required for diatomic gases. As can be seen in this figure, the heat capacity converges to its constant pressure value for the low Kn cases, and to the Knudsen heat capacity as Kn increases. The best agreement between MD results and theory is obtained with Loyalka's[18] data, except for $Kn = 10$, where the best agreement is with Sharipov's[14] data (although, for this Kn, the MD and Sharipov results are in any case close to Loyalka's[18] data).

Figures 5 and 6 show that differences in the fluid transport processes introduce differences in the heat capacities. In general, the results for $Kn = 0.5$ are close to the constant pressure heat capacity, c_p, while the results for $Kn = 10$ deviate from c_p by around $k_B/2$, and the heat capacity is then better represented by the Knudsen heat capacity, $c_{p/\sqrt{T}}$. Further analysis could be done for different gases, and also more Knudsen numbers for He and N_2, in order to get a detailed database of the heat capacities.

For hydrogen gas, MD simulations are run for two different temperature ranges: 10–100 K, and 300–500 K. Hydrogen gas in the 10–100 K temperature range can be considered as para hydrogen, and in 300–500 K it is considered as an ortho:para hydrogen mixture with the ratio 3:1. Therefore, the simulation results in the low temperature range are analyzed using Eqs. (22)–(25), while they are analyzed in the high temperature range using Eqs. (22)–(24) and (26). The results are presented in Figure 7.

The theoretical results presented in Figure 7 for constant pressure heat capacity c_p, are obtained from Eqs. (23), (25), and (26) at 10 kPa pressure. Our MD simulations are run in rarefied conditions; $Kn \approx 2.5$ for the para hydrogen case (10–100 K), and $Kn \approx 10$ for the ortho:para (3:1) hydrogen case (300–500 K). A pressure of 10 kPa in the centre of the simulated channel is obtained in both cases, making the results comparable. The comparison with the theoretical calculations enables us to check the difference between the Knudsen heat capacity and the constant pressure heat capacity. As can be seen in Figure 7, the maximum difference between c_p and c_{p/T^γ} is obtained for the ortho:para hydrogen case (3:1 ratio), and is around $0.446\, k_B/m_{H_2}$. The difference is somewhat smaller than this for the para hydrogen case, especially close to 100 K. Because the ortho hydrogen case is run at $Kn \approx 10$, then $\gamma = 0.446$, while $\gamma = 0.27$ for the para hydrogen case at a lower $Kn \approx 2.5$, to keep the cases in the same pressure range.

It can also be seen from Eqs. (23) and (24) that the deviation from the constant pressure heat capacity should be around $(\gamma k_B - p\gamma b'(T))/m$ for real gases, which can be written as $\gamma k_B/m$ for ideal
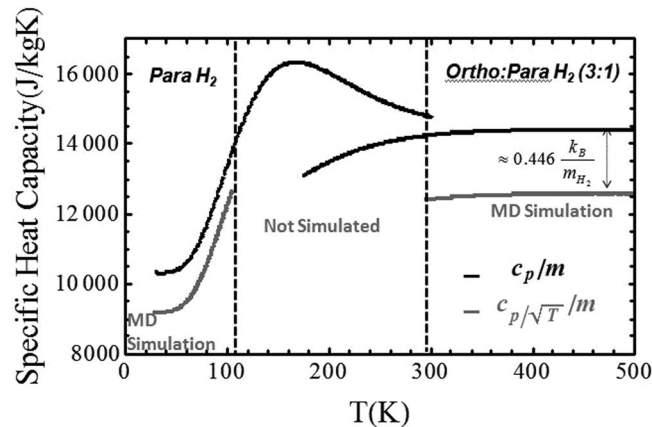
FIG. 7. Heat capacity of Hydrogen gas. The black lines are for the theoretical representation of para and ortho hydrogen in the continuum limit. The red lines represent our MD measurements in rarefied flow conditions.

gases. As γ decreases, the difference between the constant pressure and the Knudsen heat capacities becomes smaller, as we see in our results.

VII. CONCLUSIONS

We have introduced the Knudsen heat capacity for monatomic and diatomic gas systems in free molecular flow conditions, such as at the micro/nanoscale. A theoretical derivation of the Knudsen heat capacity has been presented, and validated using Molecular Dynamics simulations of nanoscale gas flows under a temperature gradient. The relationship between the Knudsen heat capacity and the well-known constant pressure heat capacity in the continuum-fluid limit can be written as $c_p - c_{p/\sqrt{T}} = k_B/2$ for ideal gases, where k_B is Boltzmann's constant. For real gases, this relationship changes depending on the intermolecular interaction potential. The Knudsen heat capacity should in general be used instead of the conventional constant pressure heat capacity to provide more realistic thermodynamic analysis when considering micro/nanoscale gas flows that follow the Knudsen law.

[1] W. A. Goddard, D. W. Brenner, S. E. Lyshevski, and G. J. Iafrate, *Handbook of Nanoscience, Engineering and Technology* (CRC Press, Boca Raton, FL, 2003).

[2] G. E. Karniadikis, N. Aluru, and A. Beskok, *Micro and Nano Flows: Fundamentals and Simulation* (Springer, New York, 2005).

[3] G. Shen, *Rarefied Gas Dynamics: Fundamentals Simulations and MicroFlows* (Springer-Verlag, Berlin, 2005).

[4] E. L. Wolf, *Nanophysics and Nanotechnology* (Wiley-VCH, Weinheim, 2004).

[5] M. Knudsen, "Eine revision der gleichgewichsbedingung der gase. Thermische Molekularstromung," Ann. Phys. **336**(1), 205 (1909).

[6] M. Knudsen, "Thermischer molekulardruck der gase in rohren," Ann. Phys. **338**, 1435 (1910).

[7] A. Sisman and I. Muller, "The Casimir-like size effects in ideal gases," Phys. Lett. A **320**, 360 (2004).

[8] A. Sisman, "Surface dependency in thermodynamics of ideal gases," J. Phys. A **37**, 11353 (2004).

[9] W. Nie and J. He, "Performance analysis of a thermosize micro/nano heat engine," Phys. Lett. A **372**, 1168 (2008).

[10] G. Babac and A. Sisman, "Thermodynamic cycles based on classical thermosize effects," J. Comput. Theor. Nanosci. **8**, 1720 (2011).

[11] G. Babac and A. Sisman, "Classical thermosize effects in degenerate quantum gases," J. Comput. Theor. Nanosci. **8**, 2331 (2011).

[12] A. Sisman and G. Babac, "Quantum size effects on classical thermosize effects," Continuum Mech. Therm. **24**, 339 (2012).

[13] F. Sharipov and V. Seleznev, "Data on internal rarefied gas flow," J. Phys. Chem. Ref. Data **27**(3), 657 (1998).

[14] F. Sharipov, "Rarefied gas flow through a long tube at any temperature ratio," J. Vac. Sci. Technol. A **14**(4), 2627 (1996).

[15] C. Cercignani and A. Daneri, "Flow of a rarefied gas between two parallel plates," J. Appl. Phys. **34**, 3509 (1963).

[16] H. Niimi, "Thermal creep flow of rarefied gas between two parallel plates," J. Phys. Soc. Jpn. **30**, 572 (1971).

[17] K. Takao, "Rarefied gas flow between two parallel plates," in *Proceedings of the Second International Symposium on Rarefied Gas Dynamics held at the University of California, Berkeley, CA, 1960*, edited by L. Talbot (Academic Press, New York, 1961), p. 465.

[18] S. K. Loyalka, "Kinetic theory of thermal transpiration and mechanocaloric effect. II," J. Chem. Phys. **63**(9), 4054 (1975).

[19] T. Ohwada, Y. Sone, and K. Aoki, "Numerical analysis of the Poiseuille and thermal transpiration flows between two parallel plates on the basis of the Boltzman equation for hard-sphere molecules," Phys. Fluids A **1**(12), 2042 (1989).

[20] R. B. Bird, W. E. Stewart, and E. N. Lightfoot, *Transport Phenomena* (John Wiley & Sons, West Sussex, 2006).

[21] A. M. Guenault, *Statistical Physics* (Routledge, New York, 1988).

[22] Y. Boutard, Ph. Ungerer, J. M. Teuler, M. G. Ahunbay, S. F. Sabater, J. Perez-Pellitero, A. D. Mackie, and E. Bourasseau, "Extension of the anisotropic united atoms intermolecular potential to amines, amides and alkanols: Application to the problems of the 2004 Fluid Simulation Challenge," Fluid Phase Equilib. **236**, 25 (2005).

[23] G. B. Macpherson and J. M. Reese, "Molecular dynamics in arbitrary geometries: Parallel evaluation of pair forces," Mol. Simul. **34**(1), 97 (2008).

[24] G. B. Macpherson, M. K. Borg, and J. M. Reese, "Generation of initial molecular dynamics configurations," Mol. Simul. **33**, 1199 (2007).

[25] M. K. Borg, G. B. Macpherson, and J. M. Reese, "Controllers for imposing continuum-to-molecular boundary conditions in arbitrary fluid flow geometries," Mol. Simul. **36**(10), 745 (2010).

[26] P. H. Hünenberger, "Thermostat algorithms for molecular dynamics simulations," Adv. Polym. Sci. **173**, 105 (2005).

[27] J. Vrabec, J. Stoll, and H. Hasse, "A set of molecular models for symmetric quadrupolar fluids," J. Phys. Chem. B **105**, 12126 (2001).

[28] H. Cheng, A. C. Cooper, G. P. Pez, M. K. Kostov, P. Piotrowski, and S. J. Stuart, "Molecular dynamics simulations on the effects of diameter and chirality on hydrogen adsorption in single walled carbon nanotubes," J. Phys. Chem. B **109**, 3780 (2005).

[29] P. Diep and J. K. Johanson, "An accurate H_2–H_2 interaction potential from first principles," J. Chem. Phys. **112**(10), 4465 (2000).

[30] T. Schnabel, *Molecular Modeling and Simulation of Hydrogen Bonding Pure Fluids and Mixtures* (Logos Verlag, Berlin, 2008).

[31] D. C. Rapaport, *The Art of Molecular Dynamics Simulation* (Cambridge University Press, Cambridge, 1997).